ORIGINAL PAPER

Predicting the preferred conformations of luteolin-4′-O-β-D-glucoside in gas phase: a comparison of two computational approaches

Yongzhi Li · Xiuhua Liu · Dong Chen · Zhichao Wei · Bo Liu

Abstract A tree-step computational approach has been applied to determine the lowest-energy conformers of luteolin-4′-O-β-D-glucoside (L4′G). Fifty-seven starting structures of the L4′G have been built, and then by performing with density functional theory (DFT) optimizations and second-order Møller-Plesset (MP2) calculations, the preferred conformations of L4′G are predicted. In order to test the accuracy of the computational approach, a hybrid Monte-Carlo multiple minimum (MCMM)/quantum mechanical (QM) approach is applied to determine the favorable conformers of L4′G. The alternative classification is employed to put similar conformations into the same catalogue according to the dihedral angles among the luteolin rings, glycosidic dihedral angles, and the orientations of hydroxyl and hydroxymethyl groups. The low-energy conformations are located after the optimizations at the HF/6-31G(d) and B3LYP/6-311+G(d) levels. Compared with the hybrid MCMM/QM approach, the tree-step computational approach not only remains accurate but also saves a lot of computing resources.

Y. Li · D. Chen (✉) · Z. Wei · B. Liu (✉)
Institute of Photo Biophysics, Physics and Electronics Department, Henan University, 475004, Kaifeng, China
e-mail: dongchen@henu.edu.cn
e-mail: boliu@henu.edu.cn

X. Liu
Key Laboratory of Natural Medicine and Immune Engineering, Henan Province 475004, Kaifeng, China

Introduction

The structural information of biomolecule is responsible for its physical and chemical properties [1]. Therefore, determining the possible structure of biomolecules is of prime importance in understanding their biological function. High-level quantum mechanical (QM) calculations can provide accurate structural information of the stable conformations [2, 3], but the computational cost is expensive. Molecular mechanics (MM) method, on the other hand, can have a cheaper calculational cost to obtain the stable conformations [4]. However, due to the limitation of MM method and the uncertain parameters in MM calculations, it is difficult to determine the preferred structures of biomolecule [5, 6]. Hybrid MM conformational search/QM calculation, which contains the full-space conformational search, the alternative classification, and the different levels of optimization, has been extensively applied to solve these problems [7–12]. Nevertheless, the conformational search generates hundreds and thousands of conformers because of the structural complexity of biomolecule, which, however, consumes large amount of calculation cost to optimize all the possible structures. Recently, the tree-step computational approach was used to establish the preferred conformations of β (1, 4)-linked lactoside [13]. A simple three-step procedure based on linkage sites, inter-ring hydrogen bonds, and co-operative intra-ring hydrogen bonds has been carried out to
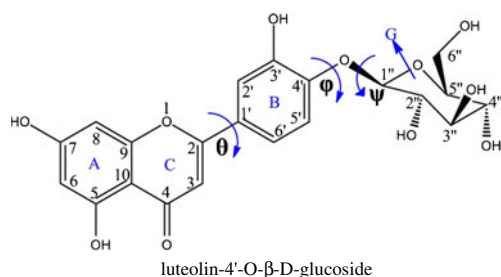
Fig. 1 Chemical structure of luteolin-4′-O-β-D-glucoside. Here, three dihedral angles (θ, φ, and ψ) have been indicated. θ=C3-C2-C1′-C2′, φ=C3′-C4′-O-C1″, ψ=C2″-C1″-O-C4′

build up starting structures of β (1, 4)-linked lactoside. Following this procedure combined with DFT optimizations and second-order Møller-Plesset (MP2) calculations, the determination process of the global minimum conformers of β (1, 4)-linked lactoside was simplified. The tree-step computational approach reduces the number of the initial structures of β (1, 4)-linked lactoside, and saves computational resources.

Based on the previous studies of disaccharide, we extend the application of the tree-step computational approach to the study of other biomolecules. Luteolin-4′-O-β-D-glucoside (L4′G), which has antibacterial [14–17], antiviral [18–20],

and antifungal [17, 21, 22] activities, was chosen to be a model molecule in this paper. Here, the tree-step computational approach was used to predict the preferred conformers of L4′G. In addition, the hybrid Monte-Carlo multiple minimum (MCMM)/quantum mechanical (QM) approach was also applied to determine the preferred conformers of L4′G. Within 4 kJ mol^{-1}, the two approaches give the same results. Comparing such two approaches of simulation of the low-energy conformations of L4′G, the tree-step computational approach simplifies the time-consuming routine procedure in the traditional strategy and radically decreases the computational cost.

Computational methods

L4′G is a type of luteolin glycosides. A glucose moiety is bound to the luteolin aglycone through one hydroxyl group (OH) at the 4′ position (see Fig. 1). Both the tree-step computational approach and the hybrid MCMM/QM approach were used to determine the preferred conformations of L4′G. In the calculation processes of the two approaches, all QM calculations were performed using Gaussian 03
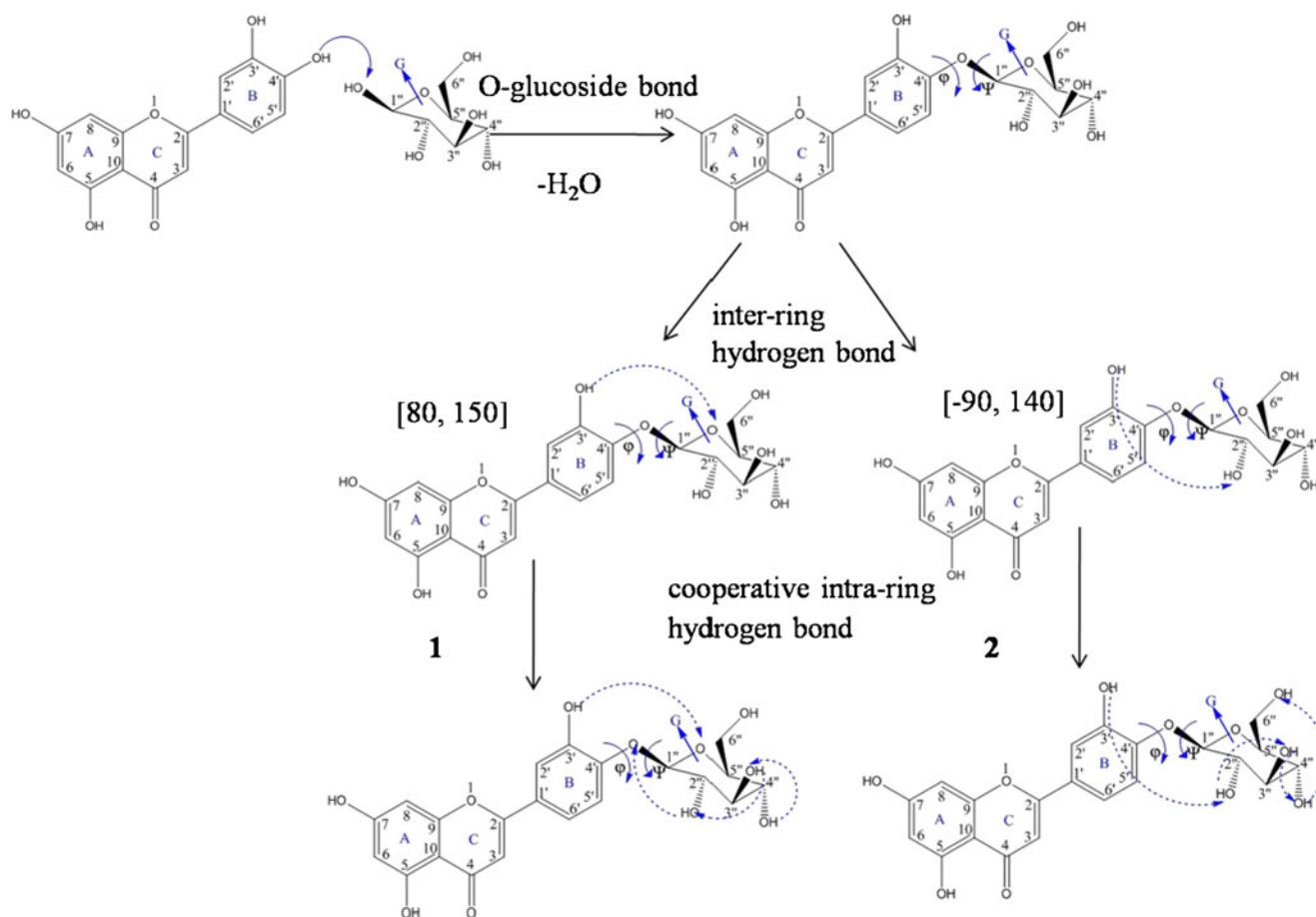

Fig. 2 Illustration of the tree-step procedure to establish two starting structures of L4′G (1 and 2)

Fig. 3 The diagram of classification procedure

software package [23]. The convergence criteria used for optimization is the default convergence criteria in Gaussian 03. The computational details of the two approaches are introduced in the following, respectively.

The computational details of the tree-step computational approach

The species diversity in inter-ring hydrogen bonds is restricted to the glycosidic linkage, and while the structural stability depends to a great extent upon inter-ring hydrogen bonds. On the other hand, the formation of cooperative intra-ring hydrogen bonds could further lower the energies [13]. Based on these, a simple procedure is used for building up starting structures, which is divided into three steps: constructing the glycosidic bond, establishing the inter-ring hydrogen bonds, and determining the cooperative intra-ring hydrogen bonds. Following the three-step procedure, 57 starting structures of L4′G were constructed in MarcoModel software [24]. Here, we chose two starting structures as an example to illustrate the construction process. The procedure is shown in Fig. 2.

Step 1: constructing the glycosidic bond. Firstly, the structures of luteolin and glucose were constructed. For the dihedral angle (θ) of the most stable conformer of luteolin, Amat et al. computed its values ranging from 11° to 34° depending on the level of theory used in vacuum [25]. Here, the dihedral angle (θ) is set to 20°. Secondly, the O-glucoside bonds are built through the OH4′ in B ring of luteolin and H1 "atom of OH1" in glucose ring. The glucose residue is connected with the B ring of luteolin residue between C4′ and C1″ sites to form glucosidic bond. Step 2: establishing the inter-ring hydrogen bonds. We focused on the inter-ring hydrogen bonds whose bond lengths are within 3 Å. Two structures, which are called structure 1 and 2, can be obtained when two types of inter-ring hydrogen bond (OH3′→OG and OH3′→OH2″) are established, respectively. The inter-ring hydrogen bond (OH3′→OG) is formed in structure 1 by adjusting OH3′ group and the dihedral angles (φ, ψ) which are adjusted to (80°, 150°). Here, the OG refers to O atom in the glucose ring. Similarly, the inter-ring hydrogen bond (OH3′→OH2″) is formed in structure 2 by adjusting OH3′ group, OH2″ group and the dihedral angles (φ, ψ) which are adjusted to (−90°, 140°). Step 3: determining the cooperative intra-ring hydrogen bonds. The cooperative intra-ring hydrogen bond (OH4″→OH3″→ OH2″→OR) is formed in structure 1 by adjusting OH4″, OH3″, and OH2″ groups. Here, the OR refers to O atom in

the glucose residues. In the same way, the cooperative intra-ring hydrogen bond (OH2″→OH3″→OH4″→OH6″) is formed in structure 2. Similar to the construction of structure 1 and 2, another 55 starting structures of the L4′G are built.

Then, all initial structures were carried out to optimize at the B3LYP/6-311+G(d) level. The relative energies used to find the global minimum structures were obtained from single point MP2/6-311++G(d,p) calculations, corrected for the zero-point energy (ZPE) derived from the B3LYP/6-311+ G(d) frequency calculations.

The computational details of the hybrid MCMM/QM approach

The following are the procedures of the hybrid MCMM/QM approach.

Fully conformational search

The function of conformational searches is to find the lowest-energy conformation [26]. It is quite simple to

Table 1 Main structural parameters of low-energy conformers obtained by the tree-step computational approach. The relative energies were obtained from single point MP2/6-311++G(d,p) calculations, corrected for the zero-point energy (ZPE) derived from the B3LYP/6-311+G(d)

Conf	The relative energy (kJ mol^{-1})	The length of inter-ring bond(Å)	θ (°)	φ (°)	ψ (°)
1	0	1.96, 2.75	159.77	85.86	163.81
2	0.02	1.95, 2.77	20.37	86.04	163.57
3	0.22	1.95, 2.77	−159.85	86.09	163.76
4	0.27	1.95, 2.75	−21.02	85.30	163.13
5	1.17	1.96, 2.74	158.90	85.86	163.87
6	1.54	1.94, 2.76	−159.28	86.01	163.71
7	1.82	1.95, 2.56	21.51	86.08	163.79
8	2.16	1.94, 2.75	−22.42	85.19	163.14
9	2.91	1.94	157.35	−94.43	139.24
10	3.10	1.93	−20.85	−92.80	139.47
11	3.47	1.93	21.75	−91.75	139.49
12	3.61	1.86	21.01	80.31	155.07
13	3.73	1.93	−161.47	−93.19	138.83
14	4.12	1.94	156.79	−94.58	139.13
15	4.59	1.87	−158.33	79.86	154.11
16	4.78	1.94	−158.68	86.89	161.90
17	4.98	1.92	23.06	−91.42	139.35

Table 2 The number of categories and the percentage of categories relating to 4922 structures at three stages

	Stage 1	Stage 2	Stage 3
The number of categories	1333	719	683
The percentage of categories	27.08 %	14.61 %	13.88 %

conduct a random variational conformational search. A starting structure is chosen, random variations to selected coordinates are applied, the structure is minimized, and comparing the result with minima found during previous conformational search steps is carried out; after storing the resulting structure as a new, unique conformer or rejecting as a duplicate, the cycle is repeated; one such cycle is called a Monte Carlo (MC) step and the entire procedure as a Monte Carlo multiple minimum (MCMM) search [27].

Here, an initial structure of L4′G was generated by MarcroModel software [24]. Then, 20,000 fully random conformational searches were implemented through MCMM method with the Merk molecular force field static (MMFFs) [28]. The bond between the B and AC rings, the OH groups, the hydroxymethyl group, and the glycosidic bond were flexible and freely rotatable through 360° in the search. All searches used 100 steps per rotatable bond with an energy cutoff of 50 kJ mol^{-1} above the global energy minimum. Four thousand nine hundred twenty-two unique conformers were identified.

Alternative classification

Here, 4922 conformers were classified by Xcluster software [29]. The procedure of classification is shown in Fig. 3. Dihedral angles (θ, φ, and ψ) mainly determine the geometry of L4′G. Therefore, the dihedral angle (θ), the dihedral angle (φ), and the dihedral angle (ψ) were considered as classification criterion of the first three-level classifications. Successively, the fourth-level classification was performed

according to the orientation of the OH groups in luteolin rings. The last-level classification was on the basis of the orientation of the OH and hydroxymethyl groups in glucose ring.

Geometry optimization

After the classification, the structures with the same range of classification criterion were put into the same category. Then, each representative structure was automatically picked up from the final category by Xcluster software [29]. In order to reduce the number of unstable conformations, the representative structures were firstly submitted to full geometry pre-optimization by *ab inito* method using Hartree-Fock (HF) with the 6-31G(d) basis set. Then the resulting structures of HF pre-optimization were submitted for DFT optimization at the B3LYP/6-311+G(d) level. Eventually, MP2/6-311++G(d,p) level calculations were carried out to determine the relative energies of the optimized geometries, which were corrected for zero point energy using the frequency calculations performed at the B3LYP level with 6-311+G(d) basis sets.

Results and discussion

Results of the tree-step computational approach

After the tree-step computational calculation, the preferred structures of L4′G are predicted. The key parameters of the low-energy conformers are listed in Table 1. From Table 1, we come to the conclusion that the value of glycosidic dihedral angles (φ, ψ) is concentrated in two areas. To gain more structural information, structural analysis of the low-energy conformers is performed in the following section.

Both inter-ring hydrogen bond and cooperative intra-ring hydrogen bond are discovered in each low-energy
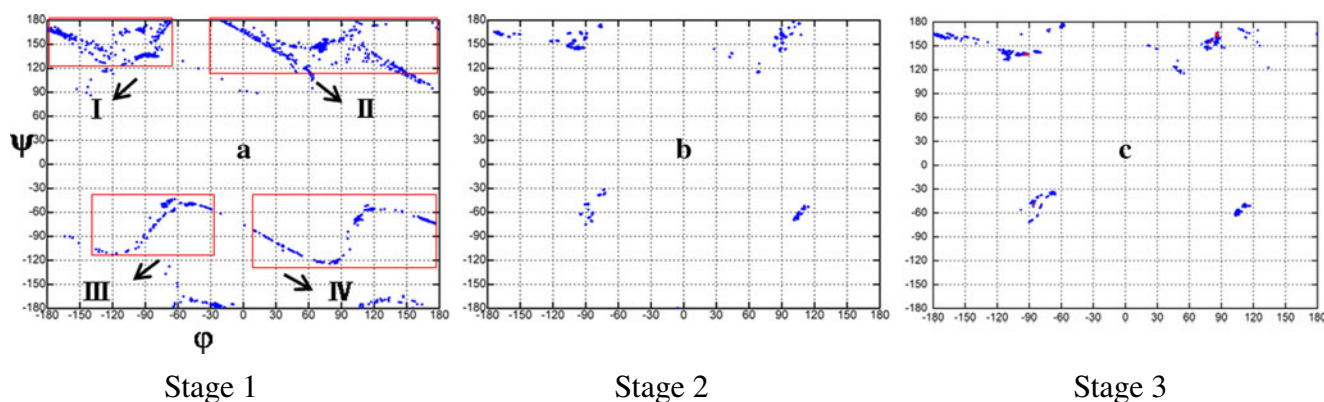

Stage 1   Stage 2   Stage 3

Fig. 4 The distribution of glycosidic dihedral angles (φ, ψ) at three stages. Stage 1: the classification procedure, stage 2: the pre-optimization at HF/6-31G(d) level, stage 3: the optimization at B3LYP/6-311+G (d) level. The dihedral angles (φ, ψ) mainly distribute in four regions I, II, III, and IV. The *red-color dots* in (**c**) indicate the distributions of the glycosidic dihedral angles for low-energy conformers within 5 kJ mol^{-1}

Fig. 5 **a** The lowest-energy conformer of L4′G and (**b**) the conformer of L4′G with energy of 16.59 kJ mol^{-1}
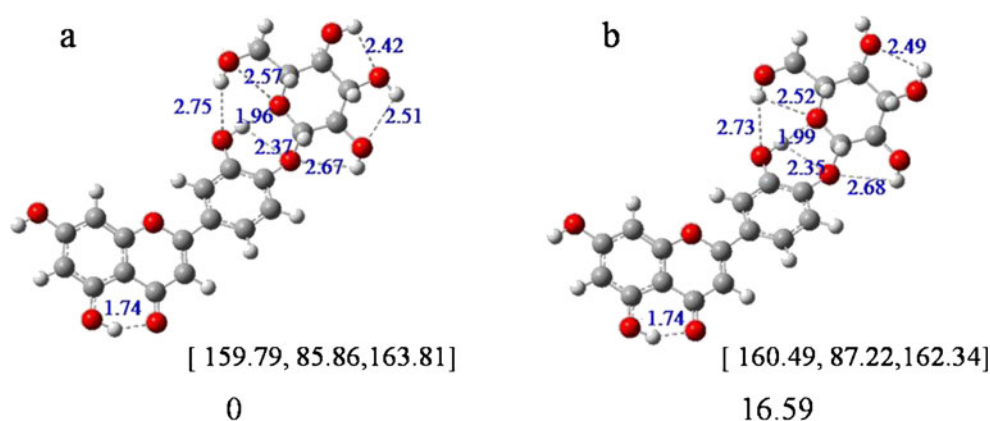
conformer. There are three types of inter-ring hydrogen bonds, which are OH3′→OG, OH6″→OH3′, and OH3′→OH2″. OH3′→OG and OH3′→OH2″, whose bonds length are between 1.9 Å and 2 Å, are strong inter-ring hydrogen bonds. OH6″→OH3′ inter-ring hydrogen bond, whose length is between 2.6 Å and 2.8 Å, is weak. The low-energy conformers involve three types of cooperative intra-ring hydrogen bonds (OH4″→OH3″→OH2″→OR, OH2″→OH3″→OH4″, and OH6″→OH4″→OH3″→OH2″→OR). These results show that inter-ring hydrogen bond and cooperative intra-ring hydrogen bond play important roles in the stabilization of certain conformers of L4′G.

Results of the hybrid MCMM/QM approach

The details of alternative classification

Firstly, 4922 conformers are generated through fully random conformational searches. These conformers can be roughly classified into five groups based on the different dihedral angle (θ), namely, group A, B, C, D, and E. Groups A, B, C, and D contain 1242, 1240, 1233, and 1119 conformers, respectively, and group E has only eight conformers. According to the dihedral angle (φ), groups A, B, C, and D are classified into 12, 12, 9, and 14 subgroups, respectively. For group E, each conformer is seen as a category. Similar to the first two levels of classification, the following three levels of classifications are carried out step by step. After five-level classification, 1333 categories are obtained. The number of categories covers 27.08 % of all the structures (see Table 2). Finally, 1333 representative structures

are automatically chosen from the corresponding categories by Xcluster software [29].

As described above, it can be drawn that despite such classification, it still takes expensive calculation cost to optimize the 1333 representative structures.

The distribution of glycosidic dihedral angles

Clearly, the glycosidic dihedral angles (φ, ψ) can characterize the spatial relation of the two rings linked by glycosidic bond. A map of the distribution of glycosidic dihedral angles (φ, ψ) in three stages has been shown in Fig. 4. The percentages of categories at the three stages are shown in Table 2.

From stage 1 to stage 2, the distribution of glycosidic dihedral angles has a significant change in each region. The percentage of categories presents a sharp reduction ranged from 27.08 % to 14.61 %. This suggests that some different conformers turn into the same structure during HF/6-31G(d) level optimization. From stage 2 to stage 3, the distribution of glycosidic dihedral angles (φ, ψ) changes a little in each region. The percentage of categories at stage 3 is 0.73 % lower than that of categories at stage 2. It indicates that there are still some different conformers to converge into identical conformer during B3LYP/6-311+G(d) level optimizations. Briefly, some unstable conformers converted into the lower energy conformers or merged into other categories during geometry optimization. The result may suggest that the spatial arrangement of atoms is re-arranged along with the change of glycosidic dihedral angles (φ, ψ), and inter-ring

Table 3 The values of the computing cost (CPU time) for each method

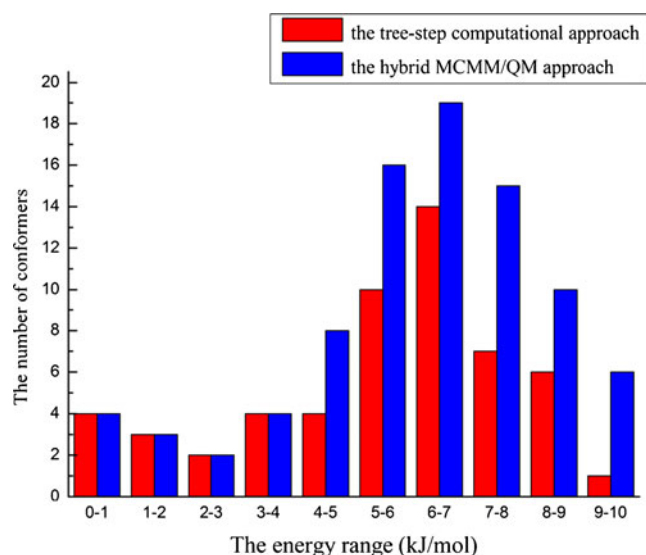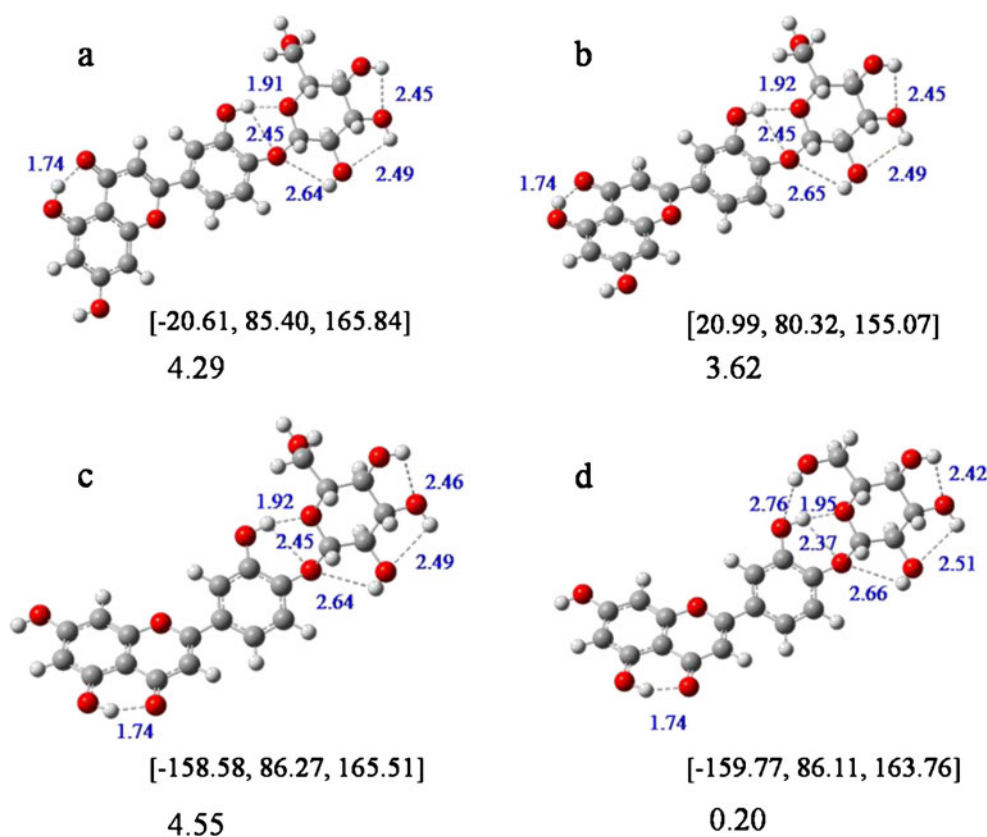|	MCMM (h)	HF optimization (h)	B3LYP optimization (h)	MP2 single point energy calculations (h)	B3LYP frequency calculations (h)	Total (h)
The tree-step computational approach			3597.76	2000.45	5776.56	11374.77
The hybrid MCMM/QM approach	1.18	8362.02	41928.17	25950.29	72649.54	148891.20

Fig. 6 The number of the conformers in different energy ranges. These conformers are both located by using the tree-step computational approach and the hybrid MCMM/QM approach

hydrogen bond and cooperative intra-ring hydrogen bond can be regenerated during the optimizations.

The distributions of the glycosidic dihedral angles for low-energy conformers within 5 kJ mol^{-1} are marked in red-color dots in Fig. 4c. It is noticeable that the glycosidic dihedral angles of low-energy conformers are mainly dispersed in two regions.

Cooperative intra-ring hydrogen bonds

The lowest-energy conformer with (θ=159.79°, φ=85.86°, and ψ=163.81°) is shown in Fig. 5a. Two typical inter-ring hydrogen bonds (OH6″→OH3′ and OH3′→OG) are observed. The intra-ring hydrogen bonds (OH6″→OG and OH5→O4) and the cooperative hydrogen bond (OH4″→OH3″→OH2″→OR) are also noticed. The conformer with energy of 16.59 kJ mol^{-1} is shown in Fig. 5b. A comparison between Fig. 5a and b shows that the two structures have similar dihedral angels (θ, φ, and ψ), inter-ring hydrogen bonds, and intra-ring hydrogen bond of OH5→O4. In Fig. 5b, OH3″ group points to OH4″ group, while OH2″ group points to OR. Because of the opposite direction of OH3″ and OH2″ groups, the hydrogen bond interaction between OH3″ and OH2″ groups could not occur. So, it is impossible to form a cooperative interaction among OH4″, OH3″, OH2″, and OR. An energy difference of 16.59 kJ mol^{-1} is caused by the lack of cooperative interactions.

Comparison of the tree-step computational approach and the hybrid MCMM/QM approach

First, let us turn our attention to the time consumption of these two approaches.

In the hybrid MCMM/QM approach, 1333 representative structures are pre-optimized at the HF/6-31G(d) level. Based on

Fig. 7 **a** The conformer with energy of 4.29 kJ mol^{-1}, **b** the conformer with energy of 3.62 kJ mol^{-1}, **c** the conformer with energy of 4.55 kJ mol^{-1}, and (**d**) the conformer with energy of 0.20 kJ mol^{-1}

the result of the HF optimization, 719 conformers' B3LYP/6-311+G(d) level optimization, single point MP2/6-311++G(d,p) calculations, and B3LYP/6-311+G(d) frequency calculations are carried out, successively. In the tree-step computational approach, only 57 starting structures are directly submitted for the B3LYP/6-311+G(d) level optimization, single point MP2/6-311++G(d,p) calculations, and the B3LYP/6-311+G(d) frequency calculations. The values of the computing cost (CPU time) for each method are listed in Table 3. Clearly, the tree-step computational approach consumes less computational resources, which reduces 92 % of the total CPU time compared to the hybrid MCMM/QM approach.

Then we compare the lowest energy conformers obtained with the two approaches. Within the energy of 5 kJ mol^{-1}, the hybrid MCMM/QM approach predicted 21 conformers, while the tree-step computational approach predicted 17 conformers and missed four conformers. The main parameters of the 17 conformers are quite close to the values obtained by the hybrid MCMM/QM approach and the tree-step computational approach. The discrepancy of the dihedral angels (θ, φ, and ψ) of the 17 conformers obtained by the two approaches is less than 0.1 %. Figure 6 shows a difference of the number of conformers between the two approaches when the energy is larger than 4 kJ mol^{-1}. Ranging from 4 kJ mol^{-1} to 10 kJ mol^{-1}, the number of conformers determined by the tree-step computational approach is less than that of the hybrid MCMM/QM approach at every energy interval of 1 kJ mol^{-1}. It results from the procedures used to construct starting structures in the tree-step computational approach. Next, we focus on two conformers which are missed in the calculations of the tree-step computational approach. The first conformer is of the relative energy of 4.29 kJ mol^{-1} shown in Fig. 7a. Compared with the conformer with the relative energy of 3.62 kJ mol^{-1} (see Fig. 7b), the difference of these two conformers exists in the dihedral angels (θ, φ, and ψ), which results in an energy difference of 0.67 kJ mol^{-1}. The other conformer is of the relative energy of 4.55 kJ mol^{-1} (see Fig. 7c). Compared with the conformer with the relative energy of 0.20 kJ mol^{-1} shown in Fig. 7d, both conformers have similar dihedral angels (θ, φ, and ψ), inter-ring hydrogen bond of OH3′→OG, and cooperative intra-ring hydrogen bond of OH4″→OH3″→OH2″→OR. The only difference is that the inter-ring hydrogen bond of OH6″→OH3′ is formed in the conformer shown in Fig. 7d, which is 4.35 kJ mol^{-1} lower in energy. The two missing conformers in the calculations prove that the tree-step computational approach concentrates on locating the lowest energy conformers. The conclusion is drawn that, in the case of L4′G, the results of the tree-step computational approach are consistent with that of the hybrid MCMM/QM approach when energy is below 4 kJ mol^{-1}, while some conformers with high energy are missing in the tree-step computational approach due to the limitation of the three-step procedure.

Conclusions

A comparison between hybrid MCMM/QM approach and tree-step computational approach clearly illustrates the advantages of the developed new modeling. Compared to the hybrid MCMM/QM approach, the tree-step computational approach simplifies calculation procedure, saves computing cost, and considerably reduces the computational time. It is important to notice that the final stable conformers located by the tree-step computational approach remains as accurate as by the hybrid MCMM/QM approach when the relative energy of conformers is within 4 kJ mol^{-1}. Therefore, the tree-step computational approach provides another option to efficiently and accurately determine the favorable geometries of biomolecules.

References

1. Seybold PG, May M, Bagal UA (1987) Molecular structure–property relationships. J Chem Educ 64:575–581
2. Strati GL, Willett JL, Momany FA (2002) Ab initio computational study of β-cellobiose conformers using B3LYP/6-311++G**. Carbohyd Res 337:1833–1849
3. Deshmukh MM, Bartolotti LJ, Gadre SR (2008) Intramolecular hydrogen bonding and cooperative interactions in carbohydrates via the molecular tailoring approach. J Phys Chem A 112:312–321
4. Asensio JL, Jimenez-Barbero J (1995) The use of the AMBER force field in conformational analysis of carbohydrate molecules: determination of the solution conformation of methyl α-Lactoside by NMR spectroscopy, assisted by molecular mechanics and dynamics calculations. Biopolymers 35:55–73
5. Engelsen SB, Koca J, Braccini I, Hervé du Penhoat C, Pérez S (1995) Travelling on the potential energy surfaces of carbohydrates: comparative application of an exhaustive systematic conformational search with an heuristic search. Carbohyd Res 276:1–29
6. Imberty A, Perez S (2000) Structure, conformation, and dynamics of bioactive oligosaccharides: theoretical approaches and experimental validations. Chem Rev 100:4567–4588
7. Jockusch RA, Kroemer RT, Talbot FO, Snoek LC, Carcabal P, Simons JP, Havenith M, Bakker JM, Compagnon I, Meijer G, von Helden G (2004) Probing the glycosidic linkage: UV and IR ion-dip spectroscopy of a lactoside. J Am Chem Soc 126:5709–5714
8. Carcabal P, Hünig I, Gamblin DP, Liu B, Jockusch RA, Kroemer RT, Snoek LC, Fairbanks AJ, Davis BG, Simons JP (2006) Building up key segments of N-glycans in the gas phase: intrinsic structural preferences of the α(1,3) and α(1,6) dimannosides. J Am Chem Soc 128:1976–1981
9. Carcabal P, Jockusch RA, Hünig I, Snoek LC, Kroemer RT, Davis BG, Gamblin DP, Compagnon I, Oomens J, Simons JP (2005) Hydrogen bonding and cooperativity in isolated and hydrated sugars: mannose, galactose, glucose, and gactose. J Am Chem Soc 127:11414–11425

10. Hünig I, Painter AJ, Jockusch RA, Carcabal P, Marzluff EM, Snoek LC, Gamblin DP, Davis BG, Simons JP (2005) Adding water to sugar: a spectroscopic and computational study of α- and β-phenylxyloside in the gas phase. Phys Chem Chem Phys 7:2474–2480

11. Carcabal P, Patsias T, Hünig I, Liu B, Kaposta C, Snoek LC, Gamblin DP, Davis BG, Simons JP (2006) Spectral signatures and structural motifs in isolated and hydrated monosaccharides: phenyl α- and β-fucopyranoside. Phys Chem Chem Phys 8:129–136

12. Su Z, Cocinero EJ, Stanca-Kaposta EC, Davis BG, Simons JP (2009) Carbohydrate–aromatic interactions: a computational and IR spectroscopic investigation of the complex, methyl α-L-fucopyranoside • toluene, isolated in the gas phase. Chem Phys Lett 471:17–21

13. Chen D, Yao YH, Wei ZC, Zhang S, Tu PH, Liu B, Dong MD (2013) Determining the structural preferences of dimannosides through the linkage constraint and hydrogen-bonded network. Comp Theor Chem 1010:45–52

14. Lv PC, Li HQ, Xue JY, Shi L, Zhu HL (2009) Synthesis and biological evaluation of novel luteolin derivatives as antibacterial agents. Eur J Med Chem 44:908–914

15. Sousa A, Ferreira IC, Calhelha R, Andrade PB, Valentao P, Seabra R, Estevinho L, Bento A, Pereira JA (2006) Phenolics and antimicrobial activity of traditional stoned table olives 'alcaparra'. Bioorg Med Chem 14:8533–8538

16. Tshikalange TE, Meyer JJM, Hussein AA (2005) Antimicrobial activity, toxicity and the isolation of a bioactive compound from plants used to treat sexually transmitted diseases. J Ethnopharmacol 96:515–519

17. Zhu XF, Zhang HX, Lo R (2004) Phenolic compounds from the leaf extract of artichoke (Cynara scolymus L.) and their antimicrobial activities. J Agric Food Chem 52:7272–7278

18. Yi L, Li ZQ, Yuan KH, Qu XX, Chen J, Wang GW, Zhang H, Luo HP, Zhu LL, Jiang PF, Chen LR, Shen Y, Luo M, Zuo GY, Hu JH, Duan DL, Nie YC, Shi XL, Wang W, Han Y, Li TS, Liu YQ, Ding MX, Deng HK, Xu XJ (2004) Small molecules blocking the entry of severe acute respiratory syndrome coronavirus into host cells. J Virol 78:11334–11339

19. Liu AL, Liu B, Qin HL, Lee SM, Wang YT, Du GH (2008) Anti-influenza virus activities of flavonoids from the medicinal plant elsholtzia rugulosa. Planta Med 74:847–851

20. Wu MJ, Weng CY, Ding HY, Wu PJ (2005) Anti-inflammatory and antiviral effects of glossogyne tenuifolia. Life Sci 76:1135–1146

21. De Campos MP, Cechinel Filho V, Da Silva RZ, Yunes RA, Zacchino S, Juarez S, Bella Cruz RC, Cruz AB (2005) Evaluation of antifungal activity of piper solmsianum C. DC. var. solmsianum (piperaceae). Biol Pharm Bull 28:1527–1530

22. Sartori MRK, Pretto JB, Cruz AB, Bresciani LFV, Yunes RA, Sortino M, Zacchino SA, Cechinel Filho V (2003) Antifungal activity of fractions and two pure compound s of flowers from Wedelia paludosa (Acmela brasiliensis) (Asteraceae). Pharmazie 58:567–569

23. Frisch MJ, Trucks GW, Schlegel HB, Scuseria GE, Robb MA, Cheeseman JR et al. farkas O, Tomasi J, Barone V, Cossi M, Cammi R, Mennucci B, Pomelli C, Adamo C, Clifford S, Ochterski J, Petersson GA, Ayala PY, Cui Q, Morokuma K, Malick DK, Rabuck AD, Raghavachari K, Foresman JB, Cioslowski J, V Rotiz J, Stefanov BB, Liu G, Liashenko A, Piskora P, Komaromi I, Gomperts R, Martin RL, Fox DJ, Keith T, AlLaham MA, Peng CY, Nanayakkara A, Gonzalez C, Challa-combe M, Gill MW, Johnson B, Chen W, Wong MW, Andres JL, Gonzalez C, Gordon MH, Replogle ES, Pople JA Gaussian, Inc., Pittsburgh PA (2003)

24. Fariborz M, Nigel GJR, Waynel CG, Rob L, Mark L, Craig C, George C, Thomas H, Still WC (1990) Macromodel—an integrated software system for modeling organic and bioorganic molecules using molecular mechanics. J Comput Chem 11:440–467

25. Amat A, Angelis FD, Sgamellotti A, Fantacci S (2008) Theoretical study of the structural and electronic properties of luteolin, apigenin and their deprotonated species. J Mol Struc-Theochem 868:12–21

26. Abagyan B, Argos P (1992) Optimal protocol and trajectory visualization for conformational searches of peptides and proteins. J Mol Biol 225:519–532

27. Chang G, Guida WC, Clark Still W (1989) An internal coordinate Monte Carlo method for searching conformational space. J Am Chen Soc 111:4379–4386

28. Halgren TA, Nachbar RB (1996) Merck molecular force field. IV. conformational energies and geometries for MMFF94*. J Comput Chem 17:587–615

29. Shenkin PS, McDonald DQ (1994) Cluster analysis of molecular conformations. J Comput Chem 15:899–916